ISSN 1027-5495. Functional Materials, 28, No.1 (2021), p. 14-21.
doi:https://doi.org/10.15407/fm28.01.14 © 2021 — STC "Institute for Single Crystals"

Structural, optical and luminescence features of Er^{3+}/Yb^{3+} co-doped sol-gel silica glasses

***I.Ya.Sulym*[1], *P.Veteska*[2], *R.Klement*[3], *Z.Hajduchova*[2], *J.Lokaj*[2], *A.Gatial*[2], *M.V.Borysenko*[1], *M.Janek*[2,4], *D.V.Gryn*[5], *M.S.Iakhnenko*[5], *A.P.Naumenko*[5]**

[1]Chuiko Institute of Surface Chemistry, National Academy of Sciences of Ukraine, Kyiv, Ukraine
[2]Faculty of Chemical and Food Technology, Slovak University of Technology, Bratislava, Slovak Republic
[3]FunGlass - Centre for Functional and Surface Functionalized Glass, TnUAD, Trencin, Slovak Republic
[4]Faculty of Natural Sciences, Comenius University, Bratislava, Slovak Republic
[5]Faculty of Physics, T.Shevchenko National University of Kyiv, Kyiv, Ukraine

Received April 20, 2020

The transparent erbium and ytterbium co-doped silica glasses having pink tint were obtained using a new variant of the sol-gel synthesis method. The amount of Er^{3+}/Yb^{3+} cations introduced into the glass was quantitatively monitored by energy dispersive X-ray analysis. The produced Er^{3+}/Yb^{3+} co-doped silica glasses (0.25–5 wt. Er_2O_3 and 2 wt. % Yb_2O_3) have a high optical homogeneity and contains OH groups in amount of 0.4–1 wt. %. Optical properties of samples were analyzed using UV-VIS absorption and luminescence spectroscopy. The changes in the luminescence spectra of glasses are related to the transitions of Er^{3+} and Yb^{3+} ions from glass matrix and correlate well with optical adsorption data. Upon excitation by a 978 nm Xe lamp, up-conversion emissions from Er^{3+} ions centered at 540 and 650 nm were greatly enhanced as the concentration of erbium oxide in the glasses increased. The proposed sol-gel synthesis method allows fabrication of the complex glass systems which have potential in the application of optoelectronic areas.

Keywords: sol-gel glasses, Er^{3+}/Yb^{3+} ions, photoluminescence, optical absorbtion.

Структурні, оптичні та люмінесцентні характеристики Er^{3+}/Yb^{3+} спільно легованих зразків золь-гель кварцового скла. *І.Я.Сулим, П.Ветеска, Р.Клемент, З.Хайдухова, Я.Локай, А.Гатіал, М.В.Борисенко, М.Янек, Д.В.Гринь, М.С.Яхненко, А.П.Науменко*

Прозорі спільно леговані ербієм та ітербієм зразки кварцового скла з рожевим відтінком одержано з використанням нового варіанту золь-гель синтезу. Кількісний вміст катіонів Er^{3+}/Yb^{3+} визначено енергодисперсійним рентгенівським аналізом. Одержані Er^{3+}/Yb^{3+} спільно леговані зразки скла (0,25–5 мас. % Er_2O_3 і 2 мас. % Yb_2O_3) мають високу оптичну однорідність та містять OH-групи в кількості 0,4–1 мас. %. Оптичні властивості зразків аналізували за допомогою УФ- та люмінесцентної спектроскопії. Зміни у спектрах люмінесценції зразків скла обумовлені електронними переходами іонів Er^{3+} та Yb^{3+} у скляній матриці і добре корелюють зі спектрами оптичного поглинання. При збудженні Xe-лампою випромінюванням 978 нм ап-конверсія іонів Er^{3+} з максимумами близько 540 і 650 нм значно посилюється зі збільшенням концентрації оксиду ербію у склі. Запропонований золь-гель метод синтезу дозволяє виготовляти складні скляні системи, які мають потенціал застосування в області оптоелектроніки.

Прозрачные совместно легированные эрбием и иттербием кварцевые стекла с розовым оттенком получены с использованием нового варианта золь-гель синтеза. Количественное содержание катионов Er^{3+}/Yb^{3+}, которые введены в стекло, определено энергодисперсионным рентгеновским (ЭДР) анализом. Полученные Er^{3+}/Yb^{3+} совместно легированные кварцевые стекла (0,25–5 масс. % Er_2O_3 и 2 масс. % Yb_2O_3) имеют высокую оптическую однородность и содержат OH-группы в количестве 0,4–1 масс. %. Оптические свойства образцов анализировали с помощью УФ- и люминесцентной спектроскопий. Изменения в спектрах люминесценции стекол обусловлены электронными переходами ионов Er^{3+} и Yb^{3+} в стеклянной матрице и хорошо коррелируют со спектрами оптического поглощения. При возбуждении Xe-лампой излучением 978 нм ап-конверсия ионов Er^{3+} с максимумами около 540 и 650 нм значительно усиливается с увеличением концентрации оксида эрбия в стеклах. Предлагаемый золь-гель метод синтеза позволяет изготавливать сложные стеклянные системы, которые имеют потенциал применения в области оптоэлектроники.

1. Introduction

Recently, the researches on rare earth (RE) doped glasses have received a considerable attention because of their applications in different advanced technology fields, such as fiber amplifiers, optoelectronic devices, lasers, sensors, colour displays, optical data storage and under water optical communication [1, 2]. The glasses doped with RE ions have several advantages such as easy preparation, large RE^{3+} ion doping capacity, large inhomogeneous line broadening, etc. [3]. Lot of work has been done on Er^{3+} doped, Yb^{3+} doped and Er^{3+}/Yb^{3+} co-doped phosphate [4], borate [5] and silica glasses [6] to increase their up-conversion luminescence efficiency, mechanical and chemical stabilities, and laser damage thresholds. The trivalent erbium is an ideal luminescent centre in visible, near- and mid-infrared spectral range thanks to its well defined transitions $\{^2H_{11/2}$ / $^4I_{15/2}$ (539 nm), $^4S_{3/2}$ / $^4I_{15/2}$ (557 nm), $^4F_{9/2}$ / $^4I_{15/2}$ (675 nm), $^4S_{3/2}$ / $^4I_{13/2}$ (852 nm), $^4I_{13/2}$ / $^4I_{15/2}$ (1500 nm), $^4I_{11/2}$ / $^4I_{13/2}$ (2900 nm) [7, 8]. However, glasses doped with single Er^{3+} exhibit a small absorption cross-section causing weak up-conversion luminescence [9]. This problem can be overcome by adding a sensitizer ion. The trivalent ytterbium ion, Yb^{3+}, exhibiting only one photoluminescence transition, $^2F_{5/2} \rightarrow {}^2F_{7/2}$, may act as an efficient sensitizer ion for Er^{3+}, due to its strong $^2F_{7/2} \rightarrow {}^2F_{5/2}$ absorption at ~ 980 nm, which has about 10 times the absorption cross section and a broader absorption peak at 980 nm than Er^{3+} [10].

It is well known that the characteristics of the stimulated emission of a rare earth ion depend on the surrounding host matrix in which the ions are incorporated [11]. Silica glass has many favorable properties as a host for RE ions due to its high UV transparency, good chemical and thermal stability, low thermal expansion and good mechanical strength [12]. Moreover, sol-gel is one of the most promising techniques for preparation of optical materials, in particular silica glasses, due to the low-temperature synthesis and the ability to control the structure and purity of the nanosilica used [13, 14]. The nanosilica has a uniform size and shape. The nano-SiO_2 powders provide more homogeneous distribution within the glass ceramic and improved properties such as chemical resistance, shrinkage and water absorption [15]. One of the problems of this technology is to ensure a uniform distribution of dopant particles in bulk samples. There is a technology for producing sol-gel glasses doped with ions of transition metals. It uses solutions of salts of some metals [16]. However, during heat treatment of xerogels, metal ions often move to the surface of bulk samples, which leads to property gradients. Earlier, our works have shown that the concentration and the properties of optically active ions (cerium, europium, and chromium) affect the luminescence and optical properties of the final glasses [14, 15, 17]. The main aim of the modified sol-gel technique for preparation of glass materials was to increase uniformity of the dopants distribution throughout the bulk of the glass material. Moreover, a homogeneous structure is formed with certain clusters of Er and Yb oxide nanoparticles, which should improve the response of the fluorescent glass. Therefore, the present study is focused on structural, optical and luminescence investigations of Er^{3+}/Yb^{3+} co-doped sol-gel silica glasses with different compositions using UV-VIS, photoluminescence spectroscopy, Fourier transform infrared spectroscopy, the energy dispersive X-ray and X-ray powder diffraction analysis.

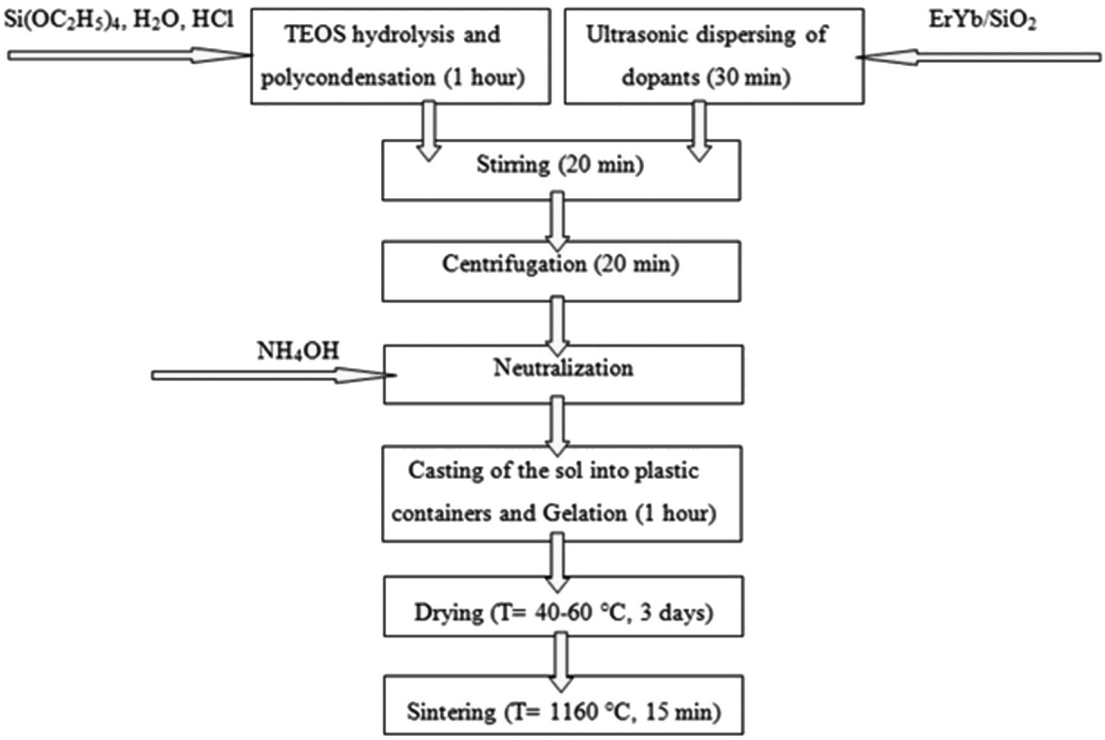

Fig. 1. Sol-gel synthesis of silica glass samples doped with Er^{3+}/Yb^{3}.

2. Experimental

A series of silica glasses containing erbium oxide (0.25–5 wt. %) and ytterbium oxide (2 wt. %) were fabricated using a modified sol-gel method. The synthesis procedure includes the following subsequent stages: i) tetraethyl orthosilicate (TEOS) hydrolysis in a three-component system $Si(OC_2H_5)_4$–H_2O–HCl with molar ratios of 1:16:0.01 with the formation of sol; ii) dispersion of doping nanopowders Er_2O_3–Yb_2O_3/SiO_2 in distilled water in an ultrasonic bath; iii) adding dispersed additives to the sol and stirring; iv) separation of coarse particles and their aggregates by centrifugation (2000 min^{-1}, 20 min); v) neutralization of the reaction mixture up to pH = 5.0 with ammonia solution (5 wt. % NH_4OH); vi) casting sol into final containers; gel curing reaction; vii) drying the gel at a temperature of 40–60°C for 3 days; viii) sintering of xerogels in air at a temperature of 1160 °C for 15 min. As a result of TEOS hydrolysis and its polycondensation, SiO_2 is formed. The weight ratio of SiO_2 produced by TEOS hydrolysis to SiO_2 in nanopowders is approximately 1:1. Consequently, the contents of Er and Yb in the prepared sol-gel glasses are 2 times less than in the initial nanopowders used. The synthesis route is schematically shown in the Fig. 1. Prepared samples were polished to get a smooth and uniform surface for optical measurements (disks diameter is about 15 mm and height – near 1.5 mm). The samples after polishing are shown in Fig. 2. The synthesis method enabled production of transparent and homogeneous materials with good mechanical properties (denoted as ErYbSi), a non-doped silica sample was used as a reference. The main difference between this production procedure and the traditional sol-gel technology is that Er and Yb ions were incorporated in the form of a nanopowder into colloidal silicon dioxide [17]. ErYbSi nanopowders (dopants) were prepared using highly dispersed fumed silica (Evonik A-300; S_{BET} = 300±30 m^2/g), and erbium and ytterbium nitrates (99.9 %, Aldrich). Er_2O_3–Yb_2O_3/SiO_2 nanopowders were prepared using a liquid-phase method. For the synthesis, aqueous salt solutions of $Er(NO_3)_3$

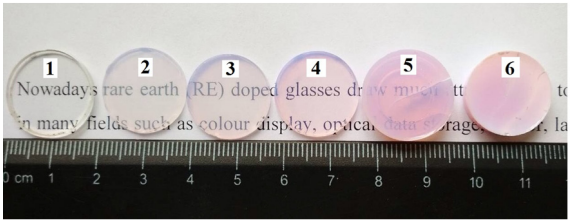

Fig. 2. Photos of pure (*1*) and co-doped sol-gel silica glasses with Er^{3+}/Yb^{3+} (2–6).

Table. EDX and FTIR analysis of Er^{3+}/Yb^{3+} co-doped silica glasses

N	Samples name	Samples composition (oxide wt. %/ mol. %)	C_{OH} (wt. %)	C (wt. %)		
				Er_2O_3	Yb_2O_3	SiO_2
1	SiO_2	SiO_2	0.3	–	–	–
2	0.25Er2YbSi	Er_2O_3(0.25/0.04)Yb_2O_3(2/0.31)SiO_2	0.9	0.27	2.38	97.35
3	0.5Er2YbSi	Er_2O_3(0.5/0.08)Yb_2O_3(2/0.31)SiO_2	0.8	0.55	2.36	97.09
4	1Er2YbSi	Er_2O_3(1/0.16)Yb_2O_3(2/0.31)SiO_2	1.0	1.26	2.91	95.83
5	2.5Er2YbSi	Er_2O_3(2.5/0.41)Yb_2O_3(2/0.32)SiO_2	0.7	5.23	4.50	90.27
6	5Er2YbSi	Er_2O_3(5/0.83)Yb_2O_3(2/0.32)SiO_2	0.4	11.4	4.74	83.83

and $Yb(NO_3)_3$ were added to 15 g fumed silica powder at room temperature. The mixtures were stirred in the beaker using a propeller stirrer for 0.5 h. Water was removed from the mixtures in a rotary evaporator. The solid was then dried and calcined at 550 °C for 1 h. The content of Er_2O_3 in the prepared nanopowders varied from 0.5 to 10 wt. % while the content of Yb_2O_3 was constant at 4 wt. %. The XRD patterns showed that all samples remained amorphous after their heating at 550 °C.

The energy-dispersive X-ray (EDX) analysis of the samples was performed by a SEM JEOL 7600-F equipped with both EDX and WDX systems.

Fourier transform infrared spectroscopy (FTIR) spectra of glasses were recorded using a Thermo Nicolet 6700 FTIR spectrometer in the range of 4000–2000 cm^{-1}. Quartz optical glass transparent in the visible region QV (Gus'-Khrustal'nyy, Russia) was used as a reference for the estimation of the content of hydroxyl groups in glasses. The Si–OH concentration (C_{OH}) was evaluated based on the measurement of the peak area under the absorption band with a maximum at 3660 cm^{-1}.

X-ray diffraction (XRD) patterns were recorded at room temperature using a DRON-3M diffractometer (Burevestnik, St.-Petersburg, Russia) with Cu K_α ($\lambda = 0.15418$ nm) radiation and a Ni filter in the 2θ range from 5 deg to 70 deg. The crystalline structure of samples was analyzed using the JCPDS Database (International Center for Diffraction Data, PA, 2001).

Optical absorption spectra UV-VIS were recorded for sol-gel silica glasses with a thickness of 190–1100 nm with a Specord 250 Plus spectrophotometer of Analytic Jena with a slit resolution of 1 nm at room temperature.

The excitation and emission fluorescence spectra were measured using Fluorolog FL3-21 and FluoroMax Plus C-P spectrometers (Horiba Jobin Yvon) with a Xe-lamp (450 W) as an excitation source. For luminescence detection in the visible spectral range, a PMT (R928, R928P) detector was used. An Optional Extended LN cooled NIR InGaAs detector was used for luminescence detection in the IR spectral range. The luminescence spectra of studied samples were recorded at room temperature (RT). The luminescence decay curves were recorded at RT with the same instrument using time correlated single photon counting (TCSPC) with a pulsed diode (Spectra LED) at an excitation wavelength of 374 nm.

3. Results and discussion

The results summarized in Table presents EDX quantitative analytical results of weight percentage of Er, Yb and Si oxides in the prepared samples. Mapping of EDX elements of Er^{3+}/Yb^{3+} co-doped samples revealed a homogeneous distribution of the dopants in the silica host matrix using the example of 1Er2YbSi glass sample (Fig. 3).

FTIR spectra for QV fused silica, pure and co-doped sol-gel silica glasses are shown in Fig. 4. A broad band with a maximum at 3660 cm^{-1} for the QV sample refers to the stretching vibrations of structural O–H bonds present in the silicon-oxygen framework. The integral absorption of OH groups in pure (Fig. 4, curve *1*) sol-gel silica glass is 3 times greater than in QV fused silica (Fig. 4, curve *QV*). It is known that the absorption is proportional to the concentration, and C_{OH} is ~ 0.1 wt. % in the QV fused glass [18], so the O–H content in pure sol-gel glass can be estimated at ~ 0.3 wt. %. The concentration of O–H groups in the co-doped glasses is greater than in pure and fused silica and varied between 0.4–1.0 wt. %

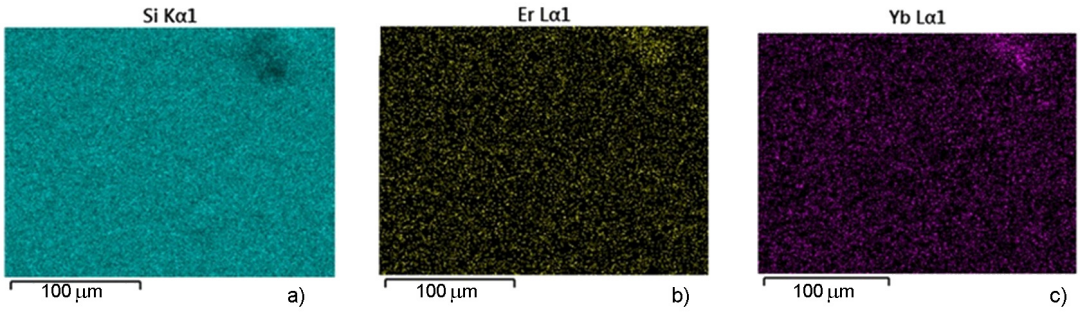

Fig. 3. EDX maps of co-doped silica glass sample (1Er2YbSi).

(Table). The concentration of hydroxyl groups in optical glasses operating at wavelengths of 0.63–1.55 μm is an important parameter, since OH groups are responsible for the absorption of radiation in this range and decrease the light penetrating intensity.

XRD patterns of pure and co-doped sol-gel silica glasses with Er^{3+}/Yb^{3+} are shown in Fig. 5. As expected, the XRD exhibits a broad scattering at 2θ = 22 deg, and confirms the amorphous nature of the prepared materials. In the case of the 5Er2YbSi sample with the maximum amount of Er^{3+}, the sharp diffraction peak in this profile (Fig. 5, curve *6*) observed at 2θ = 26.65 deg can be attributed to the crystalline phase of α-quartz SiO_2 (PDF-ICDD 86-2237). Moreover, the XRD patterns of co-doped sol-gel silica glasses with Er^{3+}/Yb^{3+} show a halo at 2θ = 32 deg which can be attributed to the amorphous silicates of erbium and ytterbium, $Er_2Si_2O_7$ (PDF-ICDD 82-0733) and $Yb_2Si_2O_7$ (PDF-ICDD 82-0734), respectively (Fig. 5, curves *2–6*).

Fig. 6 shows the absorption spectra of pure sol-gel silica glasses and sol-gel silica glasses co-doped with Er^{3+}/Yb^{3+}. The RE absorption bands originate from electronic transitions of Er^{3+} and Yb^{3+} ions from their fundamental levels to excited ones. As can be seen from Fig. 6 (curves *2–6*), the absorption spectra that exhibited bands at 358, 366, 379, 408, 444, 452, 489, 521, 546, 652, 799, and 980 nm, were due to the transition from the $^4I_{15/2}$ ground state to the excited $^2G_{7/2}$, $^4G_{9/2}$, $^4G_{11/2}$, $^4F_{9/2}$, $^4F_{3/2}$, $^4F_{5/2}$, $^4F_{7/2}$, $^2H_{11/2}$, $^4S_{3/2}$, $^4F_{9/2}$, $^4I_{9/2}$ and $^4I_{11/2}$ states of Er^{3+} ions, respectively. The absorption peaks of Yb^{3+} located at 930 and 976 nm are attributed to the transitions between different Stark levels of Yb^{3+}:$^2F_{7/2}$ and Yb^{3+}:$^2F_{5/2}$ (Fig. 6, curves *2–6*) [7, 19]. It is worth to note that the highest absorption intensity could be observed at a wavelength of 976 nm, which corresponds to the combination absorption of erbium

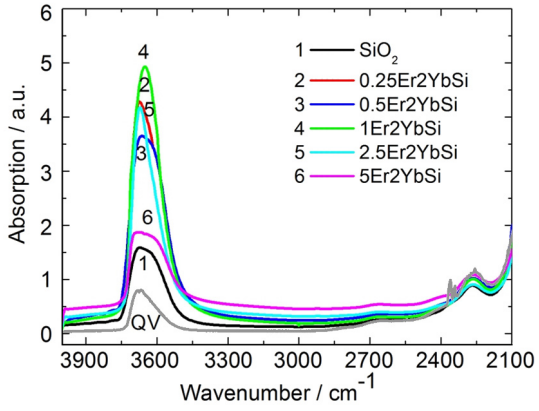

Fig. 4. FTIR spectra for QV fused silica (QV), pure (*1*) and co-doped sol-gel silica glasses with Er^{3+}/Yb^{3+} (*2–6*).

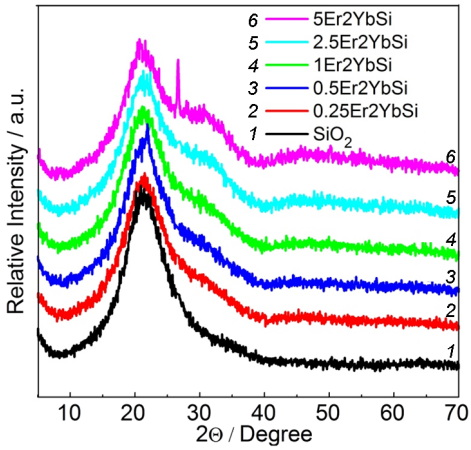

Fig. 5. XRD patterns of pure (*1*) and co-doped sol-gel silica glasses with Er^{3+}/Yb^{3}+ (*2–6*).

(transition $^4I_{15/2}\rightarrow{}^4I_{11/2}$) and ytterbium ($^2F_{7/2}\rightarrow{}^2F_{5/2}$), respectively. This attribution was reported as well in the literature [20, 21]. It can be noticed from these spectra that the intensity of the peak at 976 nm slightly decreases with the increasing amount of erbium. This may be due to the opaque character of the 2.5 Er2YbSi sample,

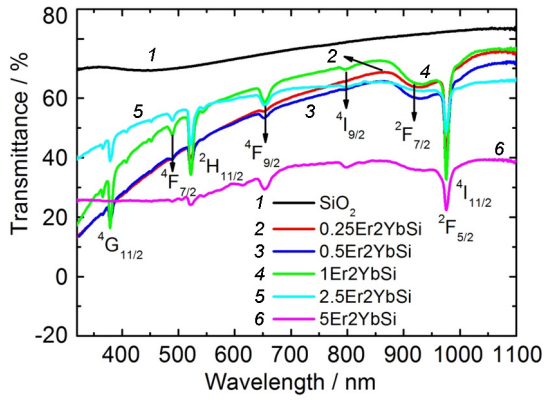

Fig. 6. UV-VIS spectra of pure (*1*) and co-doped sol-gel silica glasses with Er^{3+}/Yb^{3} (*2–6*).

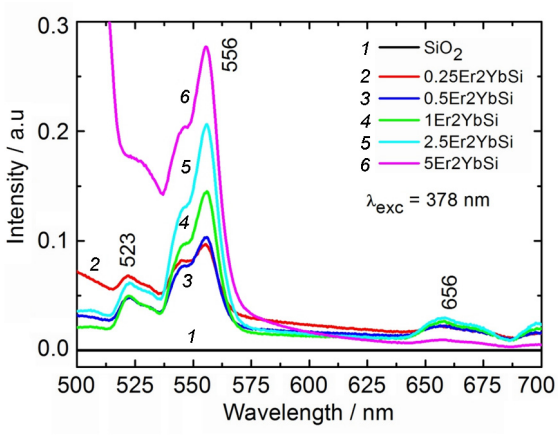

Fig. 7. Luminescence spectra of pure (*1*) and co-doped sol-gel silica glasses with Er^{3+}/Yb^{3+} (*2–6*).

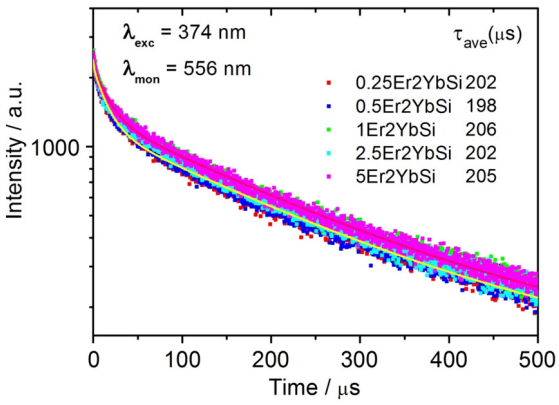

Fig. 8. Decay curves $^4S_{3/2}\rightarrow{}^4I_{15/2}$ of co-doped sol-gel silica glasses with different ratios of Er^{3+}/Yb^{3+}.

especially the sample with maximum content of Er_2O_3 (5 wt. %; 0.83 mol. %).

Fig. 7 shows the luminescence spectra in the visible range for all prepared sol-gel silica glasses excited by a source of Xe-light 378 nm. The visible emission spectra of the glasses exhibit three transitions such as $^4S_{3/2}(^2H_{11/2})\rightarrow{}^4I_{15/2}$ (green) and weak $^4F_{9/2}\rightarrow{}^4I_{15/2}$ (red) observed at 523 nm, 556 nm and 656 nm, respectively [22]. The highest intensity of green emission at 556 nm was achieved for sample (6); it was found that the intensity of red emission at 656 nm is much weaker than green emission (Fig. 7). As it can be seen from Fig. 7, the intensities of $^2H_{11/2}$, $^4S_{3/2}\rightarrow{}^4I_{15/2}$ emission transitions increase accordingly with an increase in the concentration of $Er3^+$ ions from 0.04 to 0.83 mol. %. Despite the fact, that possible clustering of Er^{3+} and Yb^{3+} ions may occur even at lower concentrations and lead to emission quenching, neither concentration quenching nor significant effect of Yb^{3+} concentration was clearly observed in the studied concentration range upon excitation at 378 nm.

The decay of the $^4S_{3/2}\rightarrow{}^4I_{15/2}$ transition for all doped silica glasses was monitored at 556 nm under 374 nm excitation (Fig. 8) and exhibit a similar profile for all studied compositions. The decay curves do not exhibit a single-exponential profile, but are well fitted (χ^2 ~ 1) with a double-exponential function (with a short decay component of ~17 μs and a long decay component of ~217 μs, respectively. Very similar decay times were found for glass samples doped with different Er^{3+} concentrations. The relative amplitude ($f_i=B_i\tau_i/\Sigma B_i\tau_i$) and the normalized pre-exponential value ($B_i/\Sigma B_i$) were found to be ~ 7 % and ~ 50 % for the short decay component and ~ 93 % and ~ 50 % for the long component, respectively. The short decay time (~ 17 μs) could be assigned to species with ion-ion (Er^{3+}–Er^{3+} and/or Er^{3+}–Yb^{3+}) interaction energy transfer through efficient cross-relaxation processes [23] and/or Er–OH centers that are present in the prepared sol-gel matrix of silica glass [24]. The average decay time ($\tau_{ave} = B_i\tau_i^2/\Sigma B_i\tau_i$) was calculated as ~ 200 μs and is shown in Fig. 8 for all compositions studied.

Up-converted luminescence spectra for Er^{3+}/Yb^{3+} co-doped sol-gel silica glasses measured using excitation of 978 nm are presented in Fig. 9. The observed green and red emission bands [25] centered at about 540 nm and 650 nm correspond to $^2H_{11/2}$,

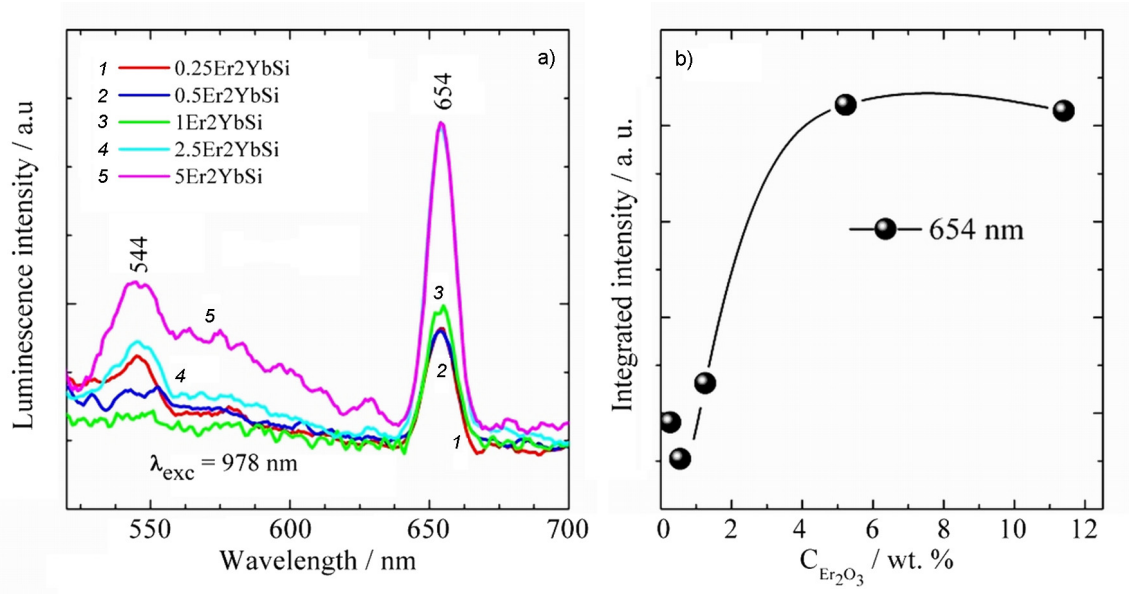

Fig. 9. Up-conversion emission (a) in co-doped sol-gel silica glasses with Er^{3+}/Yb^{3+} (*1–5*) and (b) the integrated emission intensity varying with erbium oxide concentration.

$^4S_{3/2} \rightarrow {}^4I_{15/2}$ and $^4F_{9/2} \rightarrow {}^4I_{15/2}$ transitions of Er^{3+} (Fig. 9a). As illustrated in Fig. 9b, the integrated intensities of the luminescence bands corresponding to the red transitions of Er^{3+} grow with an increase in the concentration of erbium oxide in co-doped sol-gel silica glasses.

4. Conclusions

In this work silica glasses with specified Er^{3+}/Yb^{3+} ratios were successfully prepared by a modified sol-gel technique applying co-doped SiO_2 nanopowders. All the glasses were amorphous in the nature, as confirmed by X-ray diffraction patterns, however, a crystalline phase of α-quartz SiO_2 was detected for the sample with the maximum Er^{3+} content. It was found, that the concentration of OH groups in ErYbSi glasses is 4–10 times higher than in pure and QV fused silica. The results of UV-VIS absorption spectroscopy indicated the maximum absorption intensity at 976 nm, corresponding to the combination of erbium with ytterbium in the absorption spectra of the studied glasses. As expected, the photoluminescence intensity of the prepared glasses depended on the Er^{3+}/Yb^3 ratios in the samples. The highest enhancement of green emission at 556 nm was found for the sample with the maximum erbium oxide concentration (5 wt. %; 0.83 mol. %). All the studied samples of Er^{3+}/Yb^{3+} doped silica glass exhibit a similar double-exponential decay behavior with the short decay component of ~ 17 μs and the long decay component of ~ 217 μs, respectively. In addition, upon excitation at a wavelength of 978 nm, Er^{3+}/Yb_{3+} co-doped sol-gel silica glasses exhibit intense up-conversion emission in the green and red spectral ranges. It was found that the integrated intensities of luminescence bands corresponding to the $^4F_{9/2} \rightarrow {}^4I_{15/2}$ (red) transition of trivalent Er^{3+} significantly rise with an increase in the Er_2O_3 amount in co-doped sol-gel silica glasses.

Acknowledgements. The authors acknowledge financial support by the National Scholarship Programme of the Slovak Republic supporting the study stay of Dr. I.Sulym (Contract number 19862) at Slovak University of Technology. I.S. acknowledges financial support by the Visegrad Fund (Contract number 51910525). The financial support of the Slovak Grant Agency for Science VEGA No. 1/0278/16, 1/0906/17 and 1/0527/18 are greatly appreciated. This paper is a part of dissemination activities of project FunGlass. The project has received funding from the European Union's Horizon 2020 research and innovation program under grant agreement No. 739566. This work is also based on the results of the project Center for Applied Research of New Materials and Technology Transfer, ITMS 26240220088, supported by the Science and Research Operational Program by the European Regional Development Fund.

References

1. M.Azam, R.V.Kumar, P.Mishra. *J. Mater. Sci: Mater. Electron.*, **27**, 12633 (2016).
2. L. Zhang, L.Hu, S.Jiang, *Int. J. Appl. Glass Sci.*, **9**, 90 (2018).
3. M.Sreenivasulu, A.S.Rao. *J. Mater. Sci. Lett.*, **20**, 737 (2001).
4. H.Desirena, E.De la Rosa, L.A.Diaz-Torres, G.A.Kumar. *Opt. Mater.*, **28**, 560 (2006).
5. K.Swapna, S.Mahamuda, M.Venkateswarlu et al., *J. Luminescence*, **163**, 55 (2015).
6. B.Glorieux, T.Salminen, J.Massera et al., *J, Non-Cryst. Solids*, **482**, 46 (2018).
7. K.Linganna, R.Narro-Garcia, P.Manasa et al., *J. Rare Earths*, **36**, 58 (2018).
8. S.Stanek, P.Nekvindova, B.Svecova et al., *J. Spirkova. Opt. Mater.*, **72**, 183 (2017).
9. L.X.Yi, M.Wang, S.Y.Feng et al., *Opt. Mater.*, **31**, 1586 (2009).
10. W.A.Pisarski, L.Grobelnya, J.Pisarska et al., *J. Alloys Compds.*, **509**, 8088 (2011).
11. S.Tanabe, *Int. J.*,|*Appl. Glass Sci.*. **6**, 305 (2015).
12. S.Rai, A.L.Fanai. *J. Luminescence*, **170**, 325 (2016).
13. R.Ravikumar, A.V.Chandrasekhar, L.Ramamoorthy et al., *J. Alloys Compd.*, **337**, 272 (2002).
14. M.Ignatovych, M.Borysenko, L.Davydenko et al., *Mat-wiss u Werkstofftech.*, **47**, 193 (2016).
15. M.V.Borysenko, V.M.Bogatyrov, *J. Sol-Gel Sci. Technol.*, **32**, 327 (2004).
16. K.Kajihara, *J. As. Ceram. Soc.*, **1**, 121 (2013).
17. M.V.Borysenko, K.S.Kulyk, M.V.Ignatovych et al., in: Nanomaterials and Supramolecular Structures. Physics, Chemistry, and Applications, Springer, New York (2009).
18. E.N.Poddenezhny, A.A.Boiko, Synthesis of Optical Silica Glasses, Sukhoi GGTU, Gomel (2002).
19. D.Manzani, M.Montesso, C.F.Mathias et al., *Opt. Mater.*, **57**, 71 (2016).
20. B.Lai, L.Feng, J.Wang, Q.Su, *Opt. Mater.*, **32**, 1154 (2010).
21. V.D.Rodriguez, V.K.Tikhomirov, J.Mendez-Ramos et al., *Sol. Energy Mater. Sol. Cells*, **94**, 1612 (2010).
22. K.Selvaraju, K.Marimuthu, *J. Luminescence*, **132**, 1171 (2012).
23. S.Georgescu, A.M.Voiculescu, C.Matei et al., *J. Luminescence*, **143**, 150 (2013).
24. L.T.N.Tran, D.Massella, L.Zur et al., *Appl. Sci.*, **8**, 1335 (2018).
25. W.A.Pisarski, J.Pisarska, R.Lisiecki, W.Ryba-Romanowski, *Opt. Express*, **25**, 28501 (2017).